

# On Source Identification and Alteration of Single Diesel and Wood Smoke Soot Particles in the Atmosphere; An X-Ray Microspectroscopy Study

M. G. C. VERNOOIJ,<sup>\*,†</sup> M. MOHR,<sup>†</sup>  
G. TZVETKOV,<sup>‡</sup> V. ZELENAY,<sup>‡</sup>  
T. HUTHWELKER,<sup>‡</sup> R. KAEGI,<sup>§</sup>  
R. GEHRIG,<sup>†</sup> AND B. GROBÉTY<sup>⊥</sup>

*Empa, Swiss Federal Laboratories for Materials Testing and Research, Feuerwerkerstrasse 39, Thun, CH-3602, Switzerland, Paul Scherrer Institut, EAWAG, Swiss Federal Institute of Aquatic Science and Technology, and University of Fribourg, Environmental Mineralogy*

Diesel and wood combustion are major sources of carbonaceous particles in the atmosphere. It is very hard to distinguish between the two sources by looking at soot particle morphology, but clear differences in the chemical structure of single particles are revealed by C(1s) NEXAFS (near edge X-ray absorption fine structure) microspectroscopy. Soot from diesel combustion has a dominant spectral signature at ~285 eV from aromatic  $\pi$ -bonds, whereas soot from wood combustion has the strongest signature at ~287 eV from phenolic carbon bonds. To investigate if it is possible to use these signatures for source apportionment purposes, we collected atmospheric samples with either diesel or wood combustion as a dominant particle source. No spectra obtained from the atmospheric particles completely matched the emission spectra. Especially particles from the wood dominated location underwent large modifications; the phenolic spectral signature at ~287 eV is greatly suppressed and surpassed by the peak attributed to the aromatic carbon groups at ~285 eV. Comparison with spectra from diesel soot samples experimentally aged with ozone show that very fast modification of the carbon structure of soot particles occurs as soon as they enter the atmosphere. Source attribution of single soot particles with microspectroscopy is thus hardly possible, but NEXAFS remains a powerful tool to study aging effects.

## 1. Introduction

In urban areas, carbonaceous particulate matter typically accounts for 25–50% of the ambient PM<sub>2.5</sub> (particles with a diameter <2.5  $\mu$ m (1)). Besides having a significant impact on the global climate by scattering and absorbing light (2), health effects of carbonaceous particulate matter are of great concern; high levels of PM<sub>2.5</sub> are related to increased mortality rates (3). Recent studies indicate that at similar mass

concentrations nanometer-sized particles are more toxic than micrometer-sized particles (4). Driven by episodes with very high ambient particle concentrations there is a growing public awareness of the fine particle problem and an urgent need to reduce emissions. However, efficient measures can only be taken if the different emission sources are known.

Diesel and wood combustion related particles (diameter up to a few hundreds of nanometers) are a major source of these carbonaceous particles in urban and rural areas. Consequently, distinction between the particles from these two sources is very important. Recent results (5, 6) indicate that diesel and wood combustion particles can be distinguished based on C(1s) NEXAFS (near edge X-ray absorption fine structure) on bulk material. Characteristic resonances in the spectra allow for direct molecular speciation of the graphite-like solid core, aromatic components, and surface functional groups (between ~286 and 290 eV), depending on the origin of the soot. Such detailed analyses can only be attained with NEXAFS (7). Combining NEXAFS spectroscopy and zone plate imaging, scanning transmission X-ray microscopes (STXMs) provide both high chemical sensitivity and a spatial resolution less than 40 nm which allows gaining more detailed information on the variation in structures of single soot particles depending on the combustion source. First C(1s) NEXAFS spectra were collected with X-ray microscopy in the early nineties (8). Twelve years later the technique was first used to characterize the chemical structure of soot particles from diesel combustion (9). Recently, C(1s) spectra have been published from single particles from biomass combustion (10–12) and various particles from ambient air (11, 13–15). We have investigated whether it is possible to deduce the sources (diesel or wood combustion) of single soot particles in ambient samples from C(1s) spectral information and TEM morphology. To this end we have first taken STXM based C(1s) NEXAFS spectra from individual soot particles in emission samples from test facilities (wood and diesel combustion). The spectra were used to find the characteristic bonds of single particles related to their source. Subsequently we have analyzed two PM<sub>2.5</sub> samples that were collected close to emission sources in areas where either traffic exhaust (transit road in Zurich) or wood combustion was the dominant source (Alpine village in winter). To better understand the spectra of particles in the atmospheric samples we additionally investigated the effect of particle weathering by ozone on the carbon structure. To our knowledge, this is the first study in which the chemical structure from STXM C(1s) NEXAFS spectra of single atmospheric particles are correlated with morphology from TEM images to identify particle sources.

## 2. Experimental Section

**2.1. Samples.** **2.1.1. Sample Collection.** Particles were collected on TEM silicon nitride membrane windows with 100 nm thickness (Si<sub>3</sub>N<sub>4</sub>; Silson Ltd.) using an electrostatic sampling device (16). The particles are charged in a diffusion charger, from where they are directly deposited on a TEM grid placed on a holder to which a negative voltage is applied. No previous sample treatment is necessary. Particles collected on standard filters would have to be transferred to the TEM membrane, usually requiring prior suspension in a liquid medium (9). The latter procedure is known to introduce changes in the physicochemical properties of the particles (17).

**2.1.2. Emission Samples.** Particles of two different combustion sources, wood combustion and diesel combustion, were investigated (Table 1). Diesel combustion samples were

\* Corresponding author e-mail: vernooij@alumni.ethz.ch.

<sup>†</sup> Empa.

<sup>‡</sup> Paul Scherrer Institut.

<sup>§</sup> EAWAG.

<sup>⊥</sup> University of Fribourg.

**TABLE 1. Summary of Samples Analyzed by TEM and STXM<sup>a</sup>**

	sampling conditions	particle type	dilution factor	particle concentration [#cm <sup>-3</sup> ]	sampling time [min]
Emission Samples/Diesel Combustion					
passenger car	80 kmh <sup>-1</sup>	100% soot	100×	~5 × 10 <sup>5</sup>	15
jeep	80 kmh <sup>-1</sup>	100% soot	10×	~5 × 10 <sup>6</sup>	3
truck	Medium load	100% soot	100×	~5 × 10 <sup>5</sup>	10
Emission Samples/Wood Combustion in a Simple Wood Stove					
beech wood	normal combustion	100% soot	160×	8.2 × 10 <sup>5</sup>	5
beech wood	oxygen poor combustion	100% tar balls	160×	5.0 × 10 <sup>5</sup>	10
Ambient Samples					
Zurich	winter, street canyon	mainly soot and secondary aerosols		4.1 × 10 <sup>4</sup>	afternoon Feb 5, 2007 6 h
Roveredo	winter, village, 75% of the houses are heated by wood stoves	mainly soot and secondary aerosols		3.0 × 10 <sup>4</sup>	afternoon Jan 27, 2007 3.5 h

<sup>a</sup> Particle concentrations of wood combustion samples and samples from Zurich and Roveredo were measured with a commercially available SMPS.

collected from a jeep (before Euro 1), a passenger car (Euro 4) and a truck engine (also Euro 4). All engines were operated with commercially available diesel fuel (sulfur content: <10 ppm) and were not equipped with particle filters. PM<sub>2.5</sub> wood combustion samples were collected from the chimney of a simple wood stove in which beech wood was burned under normal and oxygen poor conditions (18, 19). The water content of the wood was 20 wt % H<sub>2</sub>O, which is assumed to be an average value for wood burned in domestic wood stoves. The volatile fraction of the emissions was removed using a low-flow thermodenuder operating at 200 °C (20).

**2.1.3. Ambient Samples.** PM<sub>2.5</sub> Ambient particles were collected during the winter season at two different ambient sites (Table 1); one of the samples is dominated by vehicle exhaust, the other by wood smoke. The traffic dominated sampling site was located next to a transit road in Zurich, bordered by at least four-floored houses ("street canyon"). The wood smoke dominated site was located in Roveredo. This village is situated in the Misox, a narrow alpine valley with steep slopes at the southern side of the main alpine chain. In Roveredo 75% of the houses are heated by wood stoves. It has been shown that wood smoke is the dominant particle source (21).

**2.1.4. Artificially Aged Soot Samples.** For the particle aging experiments, four samples were collected from the jeep engine under exactly the same driving conditions as the standard jeep emission sample. The first sample was kept untreated (and later referenced as-is). The other samples were kept at room temperature in a glass tube through which a constant stream of ozone flowed (no other components were present, the tube was kept in normal sun light and was not additionally illuminated). The samples were kept in the tube for 1 min, 10 min, and 1 h, respectively. The concentration of ozone was approximately 500 μgm<sup>-3</sup>, which roughly corresponds to 10 times the maximum value of ozone during day times in January at urban locations in Switzerland. We therefore assume that the spectra of the three samples can be compared to real emission samples with residence times of 10 min, 100 min, and 10 h in the atmosphere. C(1s) NEXAFS spectra were recorded on the same day as the aging experiments had taken place.

**2.2. Analysis.** The morphology of the particles was analyzed by TEM (FEI CM30, equipped with LaB6 element, operated at 300 kV, point resolution: 0.2 nm). Imaging was performed in bright field mode. Microspectroscopy measurements were performed using the PolLux STXM microscope at the Swiss Light Source (SLS) (22). Typical STXM transmission images of atmospheric diesel or wood combustion particles recorded at 300 eV (after the C K-edge) are

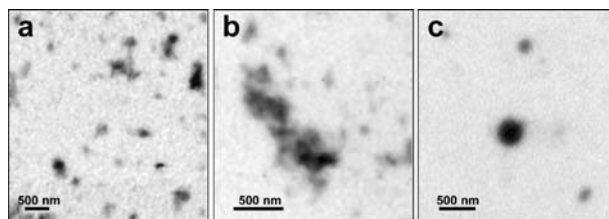


**FIGURE 1. Typical STXM transmission images at 300 eV of (a) soot from car engine, (b) wood combustion particles and (c) tar balls (see Section 3.1 for details).**

presented in Figure 1. As one can see, the zone plate limited spatial resolution of the microscope is not sufficient to investigate morphologic aspects of the particles in detail. It is however possible to distinguish particles of different types (12) and to locate them for further characterization by C(1s) NEXAFS microspectroscopy. Spectra are classified according to the presence of functional groups that were described by various authors (6, 11–15, 23, 24). The characteristic energies of individual functional groups are not strictly the same for different materials. To characterize our particles, we have therefore chosen to work with energy bands rather than specific energy values (Figures 3 and 4).

### 3. Results

**3.1. Emission Samples. 3.1.1. TEM Observations.** All three different diesel engines that were studied mainly emitted soot particles. The morphology of soot agglomerates is very well-known (25–29). Submicrometer particles consist of chains of primary particles with sizes of ~30 nm (26, 30). Primary particles have a graphitic nature with onion-like structures. The morphology of soot particles emitted from the different vehicles is similar (Figure 2a and b).

Particle types emitted from the wood stove strongly depend on the combustion conditions. If enough oxygen is provided (i.e., the shutter of the wood stove is completely open) and the fire burns already for at least 30 min, only soot particles are emitted. Ash particles (31) could not be detected in the PM<sub>2.5</sub> fraction. Soot particles from (Figure 2c) wood combustion strongly resemble soot particles from diesel combustion. The primary particles from wood combustion are though on average slightly larger (size ~40 nm (30)) than the primary particles from diesel combustion and do not exhibit a graphitic core. The sizes of the primary particles from both sources, however, show a considerable overlap which makes a discrimination of the two sources based on TEM images hardly possible.

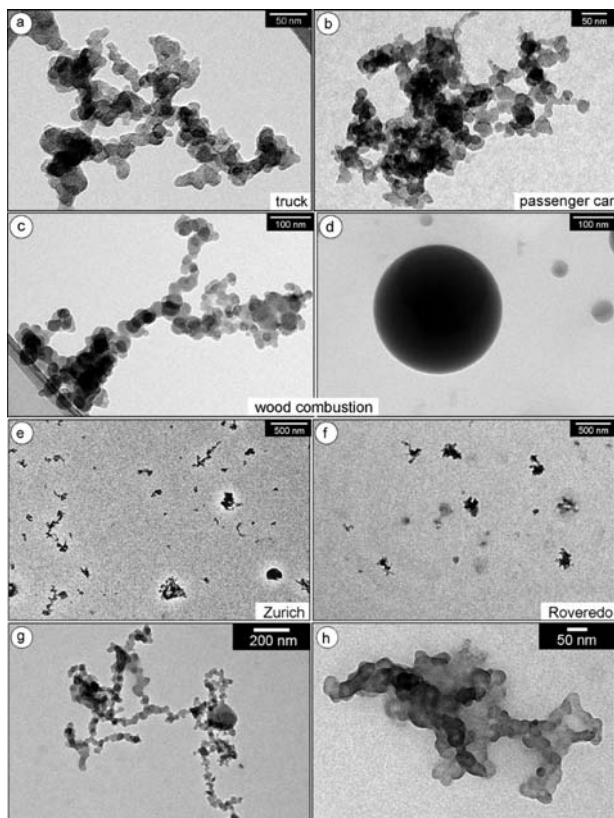


**FIGURE 2.** TEM bright field micrographs of soot from a truck engine (a), a passenger car engine (b), from wood combustion particles (c,d), and from ambient samples (e–h). The two vehicle soot particles have similar optical appearance, irrespective of their source. They both consist of aggregates of primary spherical particles that form chains. The soot particle from wood combustion (c) strongly resembles soot particles from diesel combustion. Tar balls (d) are highly spherical particles that develop in smoldering fire with a lot of smoke. The sample from Zurich (e) is mainly occupied by soot particles. The sample from Roveredo (f) shows soot particles, diffuse organic substances that form patches on the sample holder and unstable sulfate particles. Combined particles (g) are characteristic for aging. The hazy appearance of soot particle (h) is probably because of reactions with atmospheric gases and/or water.

If the shutter of the wood stove is completely closed, combustion is oxygen poor, the fire is smoldering and mainly tar balls develop (see Figure 1c and Figure 2d). Tar balls are highly spherical carbonaceous particles that have no crystallographic structure. They also develop during forest fires (12, 32). During the initial phase of combustion (approximately the first 30 min) both soot particles and tar balls develop.

**3.1.2. Carbon Spectra.** Average carbon spectra were calculated from 4 different single particle spectra for each different vehicle engine and wood combustion type (Figure 3a). The dominant signature in the spectra of all three vehicle engines is a strong peak at  $\sim 285$  eV attributed to aromatic C=C  $\pi$ -bonds and a shoulder in the spectra at  $\sim 291$  eV from equivalent C=C  $\sigma$ -bonds from the graphitic core (5). All diesel soot particles have a shoulder at  $\sim 284$  eV from benzoquinone-groups. Between 285 and 290 eV spectral features attributed to different surface functional groups can be observed. Of these, peaks of phenolic and carboxylic carbon (at  $\sim 286$  and  $\sim 288$  eV) are best developed. Small differences exist between the spectra of the different car engines. The peaks of phenolic and carboxylic carbon are more pronounced and have a higher intensity in spectra of soot particles emitted from the

jeep and the truck engine than in the spectra of soot particles from the passenger car.

The average spectrum of soot from wood combustion (Figure 3a) differs significantly from the spectra obtained from the engine exhaust particles. The aromatic peak at  $\sim 285$  eV is only very small compared to the much more pronounced phenolic carbon peak at  $\sim 287$  eV. The intensities of the aromatic, phenolic and carboxylic peaks in the tar ball spectra are approximately equal, like in diesel soot spectra, but almost twice as high.

**3.2. Ambient Samples.** **3.2.1. TEM Observations.** Most of the particles in the sample from Zurich are soot particles (Figure 2e). Within the sample from Roveredo (Figure 2f), only  $\sim 60\%$  of the particles are soot. The remaining particles are mainly organic condensates, which are not stable under the electron beam. No individual tar balls are observed. Several soot particles within the ambient samples have undergone substantial changes. Some of them are mixed with other particles like tar balls (Figure 2g) others are wrapped in a low contrast material, which gives the primary particle chains a hazy appearance (Figure 2h).

**3.2.2. Carbon Spectra.** C(1s) NEXAFS spectra were measured from over 50 particles in ambient samples. For each location, six representative spectra are shown in Figure 3b and c.

Three groups of particles are observed in the sample from Zurich. They are approximately equally present in the sample. Spectra from particles in group 1 resemble spectra of soot particles from the passenger car and jeep (Figure 3a) in the location and intensity of the peaks. The only difference is that the benzo-quinone shoulder is sometimes much more developed. This is also the case in the spectra from the particles from the second group, which are characterized by a much stronger aromatic  $\pi$ -bond peak. The main spectral features from the third group from Zurich do not coincide with any of the characteristic peaks in the emission samples and are thus most likely no soot particles. They do not show any peak or shoulder at  $\sim 285$  eV, but a very strong peak at  $\sim 286$  eV from aliphatic or ketonic carbon.

Three groups of particles can also be observed in the sample from Roveredo (Figure 3c). About 40% of the particles are of group 1, the rest is equally divided between groups 2 and 3. It is remarkable that none of the spectra in these groups resemble emission soot particle spectra from wood combustion. All spectra have a dominant peak at  $\sim 285$  eV. Spectra belonging to group 1 exhibit a steep down dipping slope between the  $\pi$ -bond and  $\sigma$ -bond aromatic peaks. Particles from group 2 also show such a slope, though this is less steep, because the peak at  $\sim 285$  eV is less high. All peaks are higher than peaks from diesel soot particles. Particles from group 3 show spectra in which intensity between 285 and 290 eV, attributed to surface functional groups, is higher than the aromatic  $\pi$ -bond peak. The intensity is also higher than in the spectra from group 1 and 2 particles in Zurich. Some of the spectra of particles in group 3 show an additional strong feature at  $\sim 286$  eV which is most likely from C=O ketone bonds. All particles from Roveredo, but especially those from group 2, show a benzo-quinone shoulder that is much more pronounced than in most of the spectra from particles in emission samples.

**3.3. Artificially Aged Soot Samples.** Ozone treatment (33) had a substantial effect on the C(1s) NEXAFS spectra from diesel soot particles (Figure 4). After only 1 min of ozone exposure, the aromatic peak is already 1.5 times higher than in the original spectrum and after 1 h it is even 2.5 times as high. The intensity of phenolic and carboxylic peaks increases 2 and 1.5 times respectively, relative to the intensity in the original spectrum. As a result, a relative steep down dipping slope develops between the  $\pi$ -bond and  $\sigma$ -bond aromatic peaks. Within the original spectra, this slope is almost

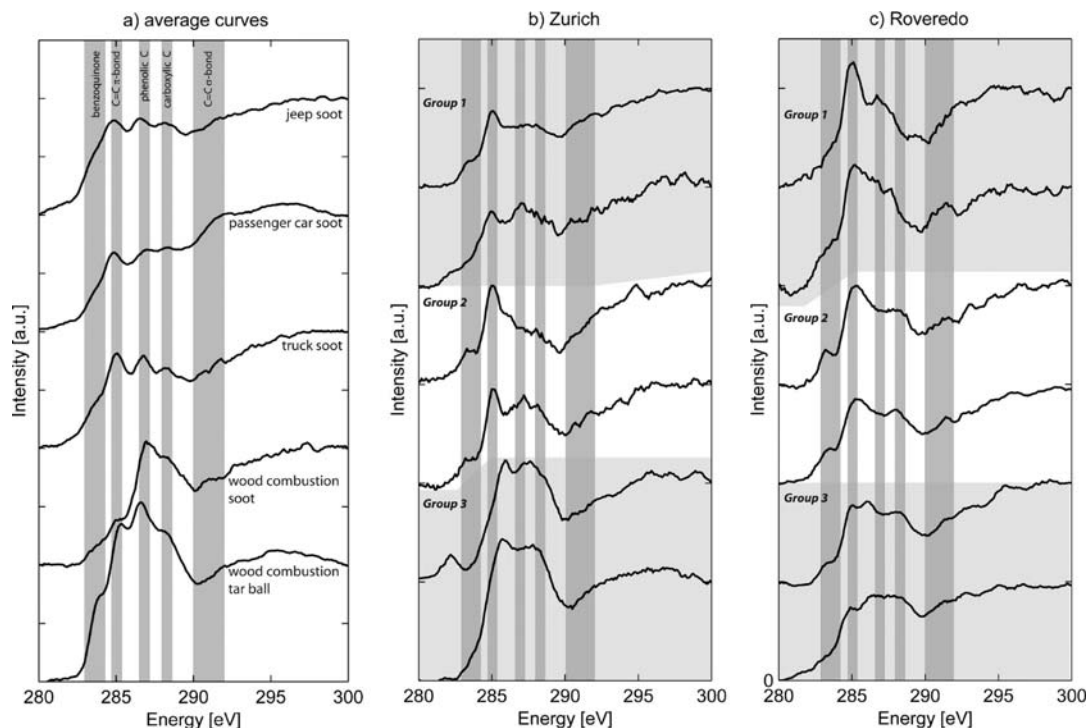


**FIGURE 3.** Average C(1s) NEXAFS spectra of soot from a jeep, a passenger car, a truck, and wood combustion and a tar ball from wood combustion (a). All spectra are averages of spectra of four particles individual. Spectra of individual particles in the samples from Zurich (b) and Roveredo (c). Three groups are defined for each sample as described in Section 3.2.2. The gray bands correspond to characteristic peaks and shoulders of the combustion particles.

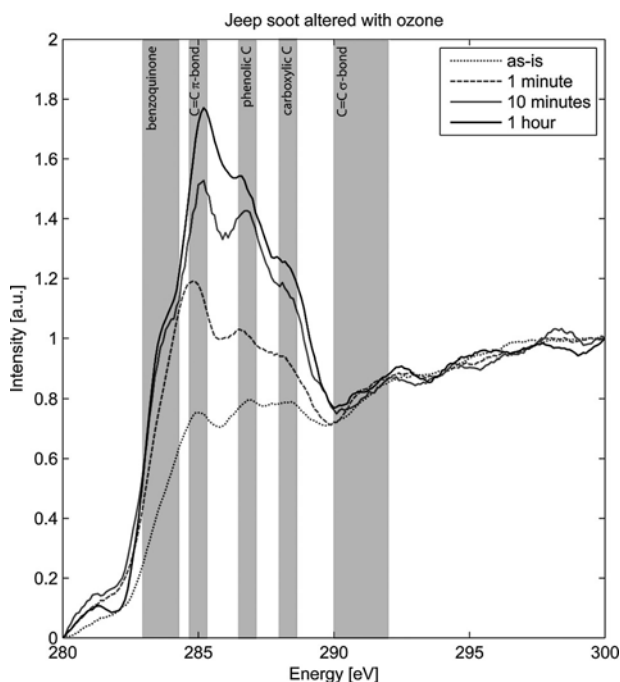


**FIGURE 4.** C(1s) NEXAFS spectra of jeep soot particles aged with ozone. All spectra are averages of spectra of four individual particles. The treatment with ozone for 1 min, 10 min, and 1 h correspond to respectively 10 min, 100 min, and 10 h in an urban atmosphere in winter.

horizontal. After 10 min in ozone, the original benzo-quinone shoulder has strongly evolved.

## 4. Discussion

**4.1. Emission Samples.** The morphological differences between soot particles from wood combustion and diesel combustion are too small to be used as distinguishing feature

(see Figure 2 and (30)). Clear differences in the nature of carbon bonding, however, can be identified (see Figure 3a). Diesel soot particles have a dominant spectral signature at  $\sim 285$  eV from aromatic C=C bonds, which corresponds to the graphitic core of the primary particles (5). Main differences between the particle spectra from the different engines are observed within the energy range in which spectral features from surface functional groups are located. The phenolic and carboxylic peaks are more pronounced for jeep and truck soot. These engines possibly release more secondary gases such as nitrous and sulfur oxides which may have reacted with the soot. The peak at  $\sim 285$  eV is only small in spectra from soot particles from wood combustion and is most likely only resulting from aromatic, but nongraphitic compounds, because of the absence of the graphitic core in the TEM observations. They show a dominant peak at  $\sim 287$  eV from phenolic C—OH bonds. The same differences have also been observed in C(1s) NEXAFS spectra from bulk samples (5, 6). Based on these observations alone, it seems to be straightforward to distinguish wood from diesel combustion derived soot particles in atmospheric samples: a possible measure to distinguish between the sources of single soot particles appears to be the intensity ratio  $I_{287 \text{ eV}}/I_{285 \text{ eV}}$  or for bulk samples the relative intensity of the aromatic peak at  $\sim 285$  eV (6). Our results on atmospheric samples, however, show that source apportionment cannot be that straightforward.

Within the particle range that can be analyzed with STXM ( $>100$  nm), only soot particles were observed in the emission samples of the diesel engines. Volatile particles, which are very common in diesel combustion samples (34) could not be detected because their size (diameter  $<50$  nm) is below the resolution limit of the STXM. Both tar balls and soot were emitted from the test facility wood stove. The increase in tar ball concentration under poorly oxygenated combustion conditions, observed in the present emission tests, has also been reported from smoldering fire (35). Our tar ball spectra, however, are different from the spectra presented by Tivanski

et al. (12), which may be explained by the difference in the type of biologic material burnt (i.e., dried wood versus life biomass).

**4.2. Atmospheric Samples.** According to the literature, both diesel and wood combustion are the most prominent sources of carbonaceous particles during winter time in Zurich (36, 37) whereas wood combustion is the dominant particle source in winter in Roveredo (21). The morphology seen in TEM images indicate that particles in the sample from Zurich with sizes larger than 100 nm are mainly soot particles. In the sample from Roveredo ~60% of the particles are soot. The fact that no tar balls are observed in this sample either means that the wood stoves are operated with enough oxygen so that no tar balls are produced, that tar balls from wood stoves are not stable in the atmosphere or that tar balls are being trapped at the chimney walls during transport into the atmosphere.

The C(1s) spectra from the particles in the ambient samples show, that the intensity ratio, proposed for the source discrimination of emission samples, is not applicable for atmospheric samples. None of the spectra have an intensity ratio  $I_{287\text{ eV}}/I_{285\text{ eV}} > 2.0$  typical for wood combustion derived particles. From the Roveredo spectra, which should contain a majority of wood combustion particles, only one spectrum had a ratio  $> 1.0$ . The spectra from the first group in the sample from Zurich are the only ones which can be compared with an emission spectra set, i.e., they strongly resemble the spectra from the diesel engine emissions. Nevertheless, even these spectra show different features than the spectra from the diesel emission samples (i.e., strong shoulder from benzoquinone bonds at ~284 eV). The spectra from the second group even show more modifications. TEM images show that some of the ambient soot particles show a modified morphology, which most likely results from particle aging (38). Aging is also the likely reason for the differences between the spectra of emission and atmospheric particles. Reaction with atmospheric gases and adsorption of new species will change the nature of the carbon bonds in particles (e.g., ref 39). This is very well illustrated by the ozone aging experiments of jeep soot emission samples. After only 10 min in ozone, the aromatic C=C peak at 285 eV of the carbon spectra is already 1.5 times higher than in the untreated soot samples, much like in the spectra from group 2 soot particles from Zurich. A similar, but less extensive, increase of the aromatic peak was also observed on bulk diesel samples weathered in the atmosphere for 10 days by Braun et al. (2008 (6)), as well as on oxidized carbon nanotubes (also, ref 6). The explanation for this phenomenon is that amorphous carbon is preferentially oxidized, leaving behind the graphitic core of the soot as indicated by the increased height of the aromatic peak at ~285 eV. This increase is more pronounced in our ozone aging experiments compared to those of Braun et al. (6) because the experimental conditions were different in terms of sample size and ozone concentration. The small peak/shoulder in the benzo-quinone region (~284 eV) that develops in spectra of particles treated for 10 min is present in almost all group 1 and 2 spectra from Zurich. Although ozone is not the only reactive species in the atmosphere, the similarities between the spectra of the ozone treated soot particles and the atmospheric particles are striking. These experimental data and the fact that the distances between the sampling locations and the major sources were very small imply that particle aging must be a very quick process (40).

Although wood combustion is the major source of particles in Roveredo (21), none of the spectra shows similarities with the spectra obtained from wood combustion emission samples. The dominant spectral signature at ~285 eV is rather characteristic for diesel engine derived soot particles. Aging is also a likely cause to explain this reversal in the  $I_{287\text{ eV}}/I_{285\text{ eV}}$  ratio. Although the aging experiments were done on diesel

engine derived particles, it can be expected that similar processes will also affect wood combustion particles. The most likely candidates for wood combustion derived particles in Roveredo are in group 3, because the aromatic peak is lower than the peaks from surface functional groups. Group 1 particles are most likely modified diesel soot particles. The high aromatic peak must have developed from an already pronounced precursor peak at the same energy (like group 2 particles from Zurich). The sources of group 2 particles from Roveredo cannot be assigned to either diesel or wood combustion. It is, however, sure that the particles are related to these combustion processes, because the characteristic peaks are the same. Aerosols generated from burning different plant fuels have different spectral characteristics (10).

Even though the spectral characteristics of soot from diesel and wood combustion emissions are very distinct, it is not possible for the Zürich and Roveredo sites to unequivocally assign particle sources by means of NEXAFS spectra. Aging is the most likely reason for the discrepancies between emission and atmospheric samples. The synchrotron based STXM technique, however, is an excellent tool to study chemical reactions during aging processes of individual submicrometer-sized soot particles, i.e., characteristic NEXAFS features can be used to follow changes and differences during reactions with atmospheric gases.

## Supporting Information Available

Details regarding engines operation and STXM details.

## Literature Cited

- (1) Hueglin, C.; Gehrig, R.; Baltensperger, U.; Gysel, M.; Monn, C.; Vonmont, H. Chemical characterisation of PM<sub>2.5</sub>, PM<sub>10</sub> and coarse particles at urban, near-city and rural sites in Switzerland. *Atmos. Environ.* **2005**, *39* (4), 637–651.
- (2) Chameides, W. L.; Bergin, M. Climate change - Soot takes center stage. *Science* **2002**, *297* (5590), 2214–2215.
- (3) Laden, F.; Schwartz, J.; Speizer, F. E.; Dockery, D. W. Reduction in fine particulate air pollution and mortality - Extended follow-up of the Harvard six cities study. *Am. J. Respir. Crit. Care Med.* **2006**, *173* (6), 667–672.
- (4) Oberdörster, G.; Oberdörster, E.; Oberdörster, J. Nanotoxicology: An emerging discipline evolving from studies of ultrafine particles. *Environ. Health Perspect.* **2005**, *113* (7), 823–839.
- (5) Braun, A. Carbon speciation in airborne particulate matter with C(1s) NEXAFS spectroscopy. *J. Environ. Mon.* **2005**, *7*(11), 1059–1065.
- (6) Braun, A.; Huggins, F. E.; Kubátová, A.; Wirick, S.; Maricq, M. M.; Mun, B. S.; McDonald, J. D.; Kelly, K. E.; Shah, N.; Huffman, G. P. Toward distinguishing woodsmoke and diesel exhaust in ambient particulate matter. *Environ. Sci. Technol.* **2008**, *42*, 374–380.
- (7) Braun, A.; Huggins, F. E.; Shah, N.; Chen, Y.; Wirick, S.; Mun, S. B.; Jacobsen, C.; Huffman, G. P. Advantages of soft X-ray absorption over TEM-EELS for solid carbon studies—a comparative study on diesel soot with EELS and NEXAFS. *Carbon* **2005**, *43*, 117–124.
- (8) Ade, H.; Zhang, X.; Cameron, S.; Costello, C.; Kirz, J.; Williams, S. Chemical contrast in X-ray microscopy and spatially resolved xanes spectroscopy of organic specimens. *Science* **1992**, *258* (5084), 972–975.
- (9) Braun, A.; Shah, N.; Huggins, F. E.; Huffman, G. P.; Wirick, S.; Jacobsen, C.; Kelly, K.; Sarofim, A. F. A study of diesel PM with X-ray microspectroscopy. *Fuel* **2004**, *83* (7–8), 997–1000.
- (10) Hopkins, R. J.; Lewis, K.; Desyaterik, Y.; Wang, Z.; Tivanski, A. V.; Arnott, W. P.; Laskin, A.; Gilles, M. K. Correlations between optical, chemical and physical properties of biomass burn aerosols. *Geophys. Res. Lett.* **2007**, *34*, (18), L18806.
- (11) Hopkins, R. J.; Tivanski, A. V.; Marten, B. D.; Gilles, M. K. Chemical bonding and structure of black carbon reference materials and individual carbonaceous atmospheric aerosols. *J. Aerosol. Sci.* **2007**, *38* (6), 573–591.
- (12) Tivanski, A. V.; Hopkins, R. J.; Tyliczek, T.; Gilles, M. K. Oxygenated interface on biomass burn tar balls determined by single particle scanning transmission X-ray microscopy. *J. Phys.*

- Chem. A* **2007**, *111* (25), 5448–5458.
- (13) Russell, L. M.; Maria, S. F.; Myneni, S. C. B. Mapping organic coatings on atmospheric particles. *Geophys. Res. Lett.* **2002**, *29* (16), 1779.
- (14) Maria, S. F.; Russell, L. M.; Gilles, M. K.; Myneni, S. C. B. Organic aerosol growth mechanisms and their climate-forcing implications. *Science* **2004**, *306* (5703), 1921–1924.
- (15) Takahama, S.; Gilardoni, S.; Russell, L. M.; Kilcoyne, A. L. D. Classification of multiple types of organic carbon composition in atmospheric particles by scanning transmission X-ray microscopy analysis. *Atmos. Environ.* **2007**, *41* (40), 9435–9451.
- (16) Fierz, M.; Kaegi, R.; Burtscher, H. Theoretical and experimental evaluation of a portable electrostatic TEM sampler. *Aerosol Sci. Technol.* **2007**, *41* (5), 520–528.
- (17) Berube, K. A.; Jones, T. P.; Williamson, B. J.; Winters, C.; Morgan, A. J.; Richards, R. J. Physicochemical characterisation of diesel exhaust particles: Factors for assessing biological activity. *Atmos. Environ.* **1999**, *33* (10), 1599–1614.
- (18) Klippel, N.; Nussbaumer, T. *Einfluss der Betriebsweise auf die Partikelemissionen von Holzöfen*; Umwelt, B. f. E. u. B. f.; Projektzusatz 1 + 2 zum Projekt Wirkung von Verbrennungspartikeln: Switzerland, 2007; ISBN 3-908705-16-9.
- (19) Klippel, N.; Nussbaumer, T. *Wirkung von Verbrennungspartikeln - Vergleich der Umweltrelevanz von Holzfeuerungen und Dieselmotoren*; Bundesamt für Energie und Bundesamt für Umwelt: Switzerland, 2007; available at <http://www.bfe.admin.ch/dokumentation/energieforschung/index.html?lang=de&publication=9137>.
- (20) Fierz, M.; Vernooij, M. G. C.; Burtscher, H. An improved low-flow thermomodulator. *J. Aerosol Sci.* **2007**, *38* (11), 1163–1168.
- (21) Alfara, M. R.; Prevot, A. S. H.; Szidat, S.; Sandradewi, J.; Weimer, S.; Lanz, V. A.; Schreiber, D.; Mohr, M.; Baltensperger, U. Identification of the mass spectral signature of organic aerosols from wood burning emissions. *Environ. Sci. Technol.* **2007**, *41* (16), 5770–5777.
- (22) Raabe, J.; Tzvetkov, G.; Flechsig, U.; Böge, M.; Jaggi, A.; Sarafimov, B.; Vernooij, M. G. C.; Huthwelker, T.; Ade, H.; Kilcoyne, D.; et al. PolLux: A new facility for soft X-Ray spectromicroscopy at the SLS. *Rev. Sci. Instrum.* **2008**, *79* (11), 113704-1–113704-10.
- (23) Cody, G. D.; Botto, R. E.; Ade, H.; Behal, S.; Disko, M.; Wirick, S. C.-NEXAFS microanalysis and scanning-X-ray microscopy of microheterogeneities in a high-volatile bituminous coal. *Energy Fuels* **1995**, *9* (1), 75–83.
- (24) Schumacher, M.; Christl, I.; Scheinost, A. C.; Jacobsen, C.; Kretzschmar, R. Chemical heterogeneity of organic soil colloids investigated by scanning transmission X-ray microscopy and C-1s NEXAFS microspectroscopy. *Environ. Sci. Technol.* **2005**, *39* (23), 9094–9100.
- (25) Chen, Y. Z.; Shah, N.; Braun, A.; Huggins, F. E.; Huffman, G. P. Electron microscopy investigation of carbonaceous particulate matter generated by combustion of fossil fuels. *Energy Fuels* **2005**, *19* (4), 1644–1651.
- (26) Mathis, U.; Mohr, M.; Kaegi, R.; Bertola, A.; Boulouchos, K. Influence of diesel engine combustion parameters on primary soot particle diameter. *Environ. Sci. Technol.* **2005**, *39* (6), 1887–1892.
- (27) van Poppel, L. H.; Friedrich, H.; Spinsby, J.; Chung, S. H.; Seinfeld, J. H.; Buseck, P. R. Electron tomography of nanoparticle clusters: Implications for atmospheric lifetimes and radiative forcing of soot. *Geophys. Res. Lett.* **2005**, *32* (24), L24811.
- (28) Kis, V. K.; Posfai, M.; Labar, J. L. Nanostructure of atmospheric soot particles. *Atmos. Environ.* **2006**, *40* (29), 5533–5542.
- (29) Adachi, K.; Chung, S. H.; Friedrich, H.; Buseck, P. R. Fractal parameters of individual soot particles determined using electron tomography: Implications for optical properties. *J. Geophys. Res., [Atmos.]* **2007**, *112*, (D14), D14202.
- (30) Kocbach, A.; Johansen, B. V.; Schwarze, P. E.; Namork, E. Analytical electron microscopy of combustion particles: a comparison of vehicle exhaust and residential wood smoke. *Sci. Total Environ.* **2005**, *346* (1–3), 231–243.
- (31) Hueglin, C.; Gaegauf, C.; Kunzel, S.; Burtscher, H. Characterization of wood combustion particles: Morphology, mobility, and photoelectric activity. *Environ. Sci. Technol.* **1997**, *31* (12), 3439–3447.
- (32) Posfai, M.; Gelencser, A.; Simonics, R.; Arato, K.; Li, J.; Hobbs, P. V.; Buseck, P. R., Atmospheric tar balls: Particles from biomass and biofuel burning. *J. Geophys. Res., [Atmos.]* **2004**, *109*, (D6), D06213.
- (33) Poschl, U.; Letzel, T.; Schauer, C.; Niessner, R. Interaction of ozone and water vapor with spark discharge soot aerosol particles coated with benzo[a]pyrene: O-3 and H2O adsorption, benzo[a]pyrene degradation, and atmospheric implications. *J. Phys. Chem. A* **2001**, *105* (16), 4029–4041.
- (34) Mathis, U.; Kaegi, R.; Mohr, M.; Zenobi, R. TEM analysis of volatile nanoparticles from particle trap equipped diesel and direct-injection spark-ignition vehicles. *Atmos. Environ.* **2004**, *38* (26), 4347–4355.
- (35) Hoffer, A.; Gelencser, A.; Guyon, P.; Kiss, G.; Schmid, O.; Frank, G. P.; Artaxo, P.; Andreae, M. O. Optical properties of humic-like substances (HULIS) in biomass-burning aerosols. *Atmos. Chem. Phys.* **2006**, *6*, 3563–3570.
- (36) Szidat, S.; Jenk, T. M.; Synal, H. A.; Kalberer, M.; Wacker, L.; Hajdas, I.; Kasper-Giebl, A.; Baltensperger, U., Contributions of fossil fuel, biomass-burning, and biogenic emissions to carbonaceous aerosols in Zurich as traced by C-14. *J. Geophys. Res., [Atmos.]* **2006**, *111*, (D7), D07206.1–D07206.12.
- (37) Lanz, V. A.; Alfara, M. R.; Baltensperger, U.; Buchmann, B.; Hueglin, C.; Szidat, S.; Wehrl, M. N.; Wacker, L.; Weimer, S.; Caseiro, A.; et al. Source attribution of submicron organic aerosols during wintertime inversions by advanced factor analysis of aerosol mass spectra. *Environ. Sci. Technol.* **2008**, *42* (1), 214–220.
- (38) Shi, Z. B.; Zhang, D. Z.; Ji, H. Z.; Hasegawa, S.; Hayashi, M. Modification of soot by volatile species in an urban atmosphere. *Sci. Total Environ.* **2007**, *389* (1), 195–201.
- (39) Karcher, B.; Mohler, O.; DeMott, P. J.; Pechtl, S.; Yu, F. Insights into the role of soot aerosols in cirrus cloud formation. *Atmos. Chem. Phys.* **2007**, *7* (16), 4203–4227.
- (40) Mak, J.; Gross, S.; Bertram, A. K. Uptake of NO3 on soot and pyrenesurfaces. *Geophys. Res. Lett.* **2007**, *34*, (10), L10804.1–L10804.5.